Prepared for submission to JINST

3RD European Conference on Plasma Diagnostics (ECPD 2019)
from 6TH to 10TH May 2019
Lisbon, Portugal

Integrated Z_{eff} Analysis on the DIII-D Tokamak

K.J Callahan,[a,1] C. Chrystal,[b] B.A. Grierson,[c] S.R. Haskey,[c] W.W. Heidbrink,[a] and J.L. Herfindal,[d]

[a] *University of California, Irvine, California 92697, U.S.A.*
[b] *General Atomics, PO Box 85608, San Diego, CA 92186, U.S.A.*
[c] *Princeton Plasma Physics Laboratory, Princeton, New Jersey 08543-0451,U.S.A.*
[d] *Oak Ridge National Laboratory, Oak Ridge, TN 37830, U.S.A.*

E-mail: kjcallah@uci.edu

Abstract: Determination of effective ion charge, or Z_{eff}, from measurements of visible bremsstrahlung radiation made by multiple diagnostics is now integrated into a single analysis workflow within the plasma profile analysis module in OMFIT [Logan et. al. Fus. Sci. & Technol. 74 125-134 (2018)]. Measurements are made across the midplane of DIII-D with independent filterscope and spectrometer based diagnostics. Emission from 5215-5245 Å is measured by 16 filtered visible bremsstrahlung measurements (filterscopes) with a sampling rate of 20 kHz. The charge exchange recombination spectroscopy (CER) system utilizes scanning spectrometers, and typically measures emission near 5291 Å with approximately 20 active spatial views. Both Abel inversion and least squares minimization analyses are performed on these chordal measurements to infer the plasma emissivity profile with respect to magnetic flux coordinate ρ. Z_{eff} is derived from this emissivity profile from a calculation involving electron density and temperature from the Thomson scattering diagnostic. This analysis has been applied for a range of plasma conditions including L-mode, H- mode and H-mode with impurity seeding. The Z_{eff} inferred from VB data is shown to be in good agreement with the Z_{eff} computed from CER impurity density profile measurements when C^{6+} is assumed to be the dominant impurity species of the plasma. This new analysis is useful for cross checking diagnostics and measuring Z_{eff} when all important impurities cannot be monitored directly with CER measurements.

Keywords: Plasma Diagnostics - charged particle spectroscopy, Analysis and Statistical methods, Data Processing Methods

[1]Corresponding Author.

Contents

1 Introduction **1**

2 Measurement Techniques **2**

3 Integrated visible bremsstrahlung data analysis **3**

3.1 Abel Inversion 3

3.2 Least Squares Minimization 4

4 Example measurements and conclusions **4**

1 Introduction

A robust method for correctly measuring radial profiles of the plasma effective ion charge, or Z_{eff}, is of general importance to fusion science and, in particular, is needed to study the mechanisms that cause radiative collapse and fuel dilution due to impurity accumulation [1]. In the past, Z_{eff} has been calculated through techniques involving active impurity charge exchange recombination spectroscopy (CER), visible bremsstrahlung continuum (VB) spectroscopy, plasma conductivity anomaly analysis, soft x-ray continuum (SXR) spectroscopy, and residual gas analysis [2–6].

The measurement of Z_{eff} by visible bremsstrahlung spectroscopy was pioneered by Kodota at the JIPP T-II tokamak in 1980 [4]. This experimental technique was adopted at the DIII-D tokamak and has seen consistent usage since 1988 [7]. The standard technique for measuring Z_{eff} at this facility, however, is made by assuming C^{6+} is the only significant impurity and measuring its density with impurity CER spectroscopy. In a comparative study performed by Whyte in 1998, it was determined that radial Z_{eff} profiles from impurity CER spectroscopy were more reliable than those derived from VB data due to uncertainties introduced by inversion [5]. However, this standard method for observing Z_{eff} is unreliable when multiple impurities are present. Specifically, simultaneous multi-ion impurity monitoring is needed under such circumstances, leading to density uncertainties due to many charge exchange cross sections not being readily available. Consequently, it is desirable to expand the diagnostic capabilities of DIII-D so observation of Z_{eff} from VB during impurity seeding is easy to implement and routinely possible.

Since 1998, many of the problems associated with DIII-D's observations of VB radiation have been ameliorated. These issues have been addressed though better data acquisition from the visible bremsstrahlung array's 16 mid-plane oriented sightlines by changing to a filterscope system in 2012 and enhancing this system's sampling rate to 20 kHz in 2013. Additionally, verification of filterscope measurements against both wavelength resolved impurity CER background and fast-framing camera measurements in 2010 demonstrated the usefulness of integrating CER background and VB filterscope data as a method for checking for line contamination [8].

These improvements, alongside an increasing number of impurity seeding experiments, prompted a re-evaluation of the VB Z_{eff} technique at DIII-D. In particular, an integrated analysis of visible bremsstrahlung data from both VB filterscope and impurity CER sightlines was developed for routine use in OMFITprofiles to meet this diagnostics need [9]. This paper describes the analyses used, and their verification against standard active impurity CER spectroscopy results.

2 Measurement Techniques

The impurity CER diagnostic at DIII-D measures ion densities, temperatures, and velocities using the spectral emission intensity, Doppler broadening, and Doppler shift of charge exchange line emission. Local observations of these quantities are made at the intersection of neutral beam and spectral chord paths. Typically C-VI is monitored through the n=8 $\rightarrow$ 7 charge exchange transition (5290.5 Å) since carbon is expected to be the dominant impurity via sourcing from the vessel's graphite walls. Important for this study, wavelength resolved chordal measurement of VB radiation are observed by the impurity CER system's background continuum. This quantity is determined by fitting to the spectrum of a charge exchange line, and finding the absolute value of the background.

The visible bremsstrahlung filterscope array at DIII-D observes emission between 5215-5245 Å using 16 filtered mid-plane oriented spectral chords. These continuum measurements are the second element of this integrated data set. Typical sightlines used, as well as a demonstration of the consistency between filterscope and CER background data is shown in Fig. 1.

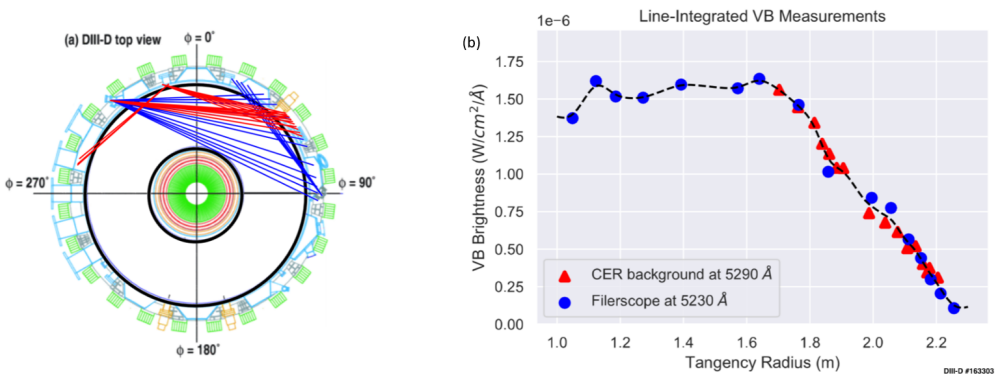

Figure 1. (a) A top down view of the DIII-D tokamak with the VB filterscope and impurity CER sightlines shown in blue and red, respectively. (b) Example VB brightness measurements with each spectral chord plotted with respect to tangency radii. In red triangles are the CER background data and in blue circles are the VB filterscope data.

It is noteworthy that CER background data is inferred by fitting and subtracting away all line radiation. Therefore, the consistency noted between filterscope and CER background data provides a direct check that filterscope data is free of line contamination. In-vessel reflection is an additional source of error since not all chords terminate at razor-viewing dumps. The sightlines shown permit the measurement of VB brightness across the entire DIII-D midplane, allowing for the experimental verification of whether impurities break flux symmetry. Since these data are chordal measurements, a line integral inversion is needed to deduce local properties.

3 Integrated visible bremsstrahlung data analysis

Multiple inversion methods were developed within the workflow for OMFITprofiles to determine Z_{eff}, with the assumption that effective ion charge is a function of magnetic flux. Analysis of integrated VB data from DIII-D's CER and VB filterscope diagnostics is accomplished by first placing these data within a framework where multiple parameters relevant to each spectral view can be recorded. These include the sightline geometries, wavelength settings, and VB brightness measurements. Using this data framework, determination of Z_{eff} from integrated VB data is accomplished one of two ways: Abel inversion or least squares minimization.

The cold plasma edge, where the VB continuum is often contaminated by molecular band pseudo-continuum and line radiation, can contribute noticeably to VB brightness measurements [10, 11]. Mantle radiation is subtracted away from each chordal measurement prior to inversion by approximating its intensity from measurements from the outermost filterscope chord, which samples only the cold edge. Accounting for mantle emission by subtraction has been performed in the past at facilities such as DIII-D, ASDEX-U, and JET [7, 12, 13].

3.1 Abel Inversion

One method of determining Z_{eff} from multiple chordal VB measurements is Abel inversion. The Abel inversion technique used is a standard matrix inversion analysis pioneered by Hörmann [14]. The result is an emissivity profile dependent on major radius R. Using equilibrium reconstruction results, this emissivity profile is mapped to spatial coordinate ρ, the square root of normalized toroidal flux, in order to combine diagnostics at multiple spatial locations. Following this variable conversion, Z_{eff} is determined from this emissivity profile ϵ_λ (W/cm^3/Å) by the following relation:

$$Z_{\text{eff}}(\rho, t) = \frac{\epsilon_\lambda(\rho, t)\ T_e^{1/2} \lambda^2}{1.89 \times 10^{-28}\ n_e^2\ g_{ff}\ exp(-12400/T_e \lambda)} \tag{3.1}$$

Here, electron temperature T_e (eV) and electron density n_e ($1/cm^3$) are measured using the Thomson Scattering diagnostic. It is assumed that these properties are constant on a flux surface. The wavelength of the continuum observed (λ) is given in Å. The free-free gaunt factor used in this workflow is $g_{ff} = 1.35\, T_e^{0.15}$ [15]. Prior to inversion, since multiple wavelengths of continuum are observed, all VB data is mapped to 5230 Å assuming a dependency of $\epsilon_\lambda \propto \lambda^{-2}$. This mapping allows many independent VB measurements to be used together when determining an emissivity profile. A Salvitzky-Golay data smoother is applied to this data set when plotted versus tangency radius as in Fig. 1(b) to minimize the effects of spurious channels [16]. This enables the inversion to be less susceptible a single channel's contamination by in-vessel reflection or line-radiation by forcing chordal measurements to be smoothly varying with sightlines on similar trajectories. Inversion errors are estimated by a Monte Carlo scheme identical to one used by Patel at MAST [11]. These inversion errors are propagated in quadrature with Thomson uncertainties to determine Z_{eff} errors. The VB brightness uncertainties, as well as Thomson errors, are determined from the standard deviation of random fluctuations in a time window where the plasma is stationary, with systematic errors not used at this time due to their difficulty to quantify. The output of this analysis is a finite number of points at various ρ, which are fit to find a continuous Z_{eff} radial profile. Because this inversion maps emission to major radius, a distinction between high and low field side

Z_{eff} can be made. As a result, Abel inversion is used to experimentally identify if Z_{eff} breaks flux symmetry. This asymmetry assessment is especially important for high-Z impurities, which have been observed to vary along flux surfaces in the past at devices such as C-Mod [17].

3.2 Least Squares Minimization

The second method implemented to determine Z_{eff} from multiple chordal VB measurements is least squares minimization. Specifically, minimization was performed using the python module LMFIT [18]. In this analysis, an initial guess for the Z_{eff} radial profile is made using one of three possible basis functions: a variable order polynomial, a manually knotted cubic spline, or a Gaussian radial basis function. With this initial guess and known T_e and n_e profiles, a model emissivity profile ϵ_λ is calculated from Eq. 3.1. For each spectral view, this emissivity profile is line integrated along each chord's path through the plasma at its set wavelength λ. These model VB brightness measurements are then compared to experimental observations, and normalized by experimental error, for each sightline at a specific time slice to calculate a set of residuals. With these residuals, a least squares minimization is performed on the initially guessed Z_{eff} by varying the basis function's free parameters. For this minimization, the Thomson profiles are taken as absolute. The least square algorithm's criteria for convergence is modified from the standard set by LMFIT to decrease computation time. The relative tolerance needed for convergence is the change of the sum of squared residuals is less than 10^{-3} when going from one iteration to the next [18]. The output from this analysis is the continuous Z_{eff} radial profile which meets this convergence criterion. Confidence bands are calculated from 1σ error estimates from the basis function's free parameters.

4 Example measurements and conclusions

Computation of Z_{eff} from VB data by Abel Inversion and Least Squares Minimization has been done for a standard L-mode, a standard H-mode, and a carbon dominated L-mode plasma. These cases demonstrate that this analysis is consistent with CER measurements of Z_{eff} for a wide range of conditions and under the assumption that C^{6+} is the only significant plasma impurity.

Analysis of a standard L-mode plasma, shown in Fig. 2(a), demonstrates how Z_{eff} radial profiles from VB data can be used to verify Z_{eff} profiles from CER analysis when only C^{6+} is monitored. In particular, this data consistency can increase confidence in absolute and relative calibrations of the impurity CER system, as well as the assumption that the plasma contains only a single dominant light impurity species. The former is important because corrections to the C^{6+} density measurements can be necessary to account for beam-based variations. These results help validate the use of such techniques in CER analysis.. Demonstration of the latter gives more confidence in the accuracy of D^+ density profiles calculated by assuming quasi-neutrality with C^{6+} as the only impurity species. Furthermore, Abel inversion results (red and purple) which are independent of either continuous profile shown are found to be symmetric about the high and low field sides, suggesting that impurity flux symmetry is valid for this particular discharge. Similar conclusions result from a comparison of Z_{eff} from VB and CER analysis for a standard H-mode plasma shown in Fig. 2(b). The least squares fitting parameters used however, limit the accuracy of Z_{eff} modeling. Furthermore, imperfect subtraction of mantle radiation leads to suspect edge Z_{eff} values. These two effects cause the VB determined Z_{eff} profile shapes to deviate from the active CER Z_{eff}.

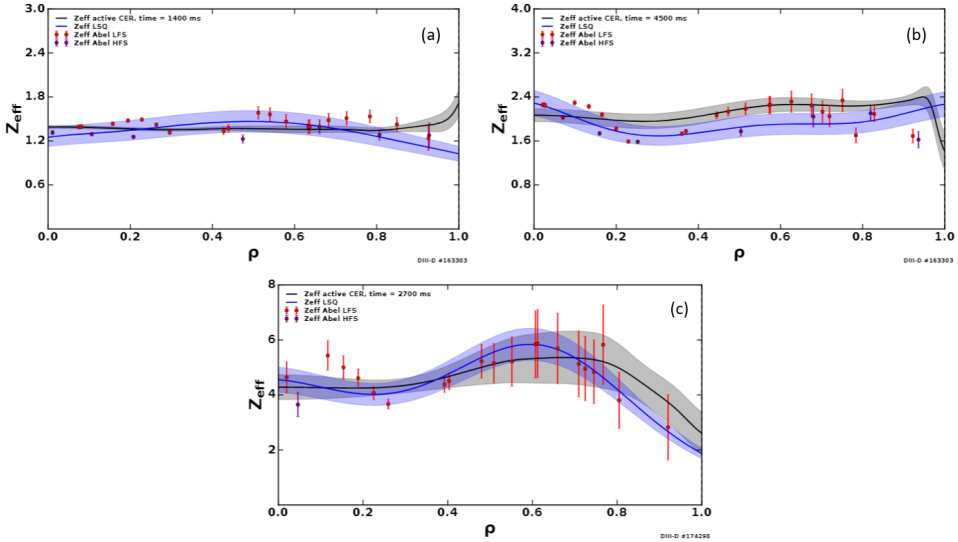

Figure 2. Z_{eff} radial profiles for a standard L-mode (a), a standard H-mode (b), and a L-mode plasma contaminated by carbon via a graphite tipped reciprocating probe (c). In black is Z_{eff} calculated from CER spectroscopy, in blue is Z_{eff} determined from VB data using least square minimization with a RBF Gaussian, and in red/purple are the discrete calculations of Z_{eff} at various ρ from Abel Inversion. 1 σ confidence bands are shown in the shaded regions in grey and blue for the LSQ and CER analyses respectively.

Analysis of a carbon dominated L-mode plasma illustrates how Z_{eff} radial profiles from VB data can be applied to unique discharges to identify plasma contamination. This discharge was formed when a graphite tipped reciprocating probe was inadvertently left inside the plasma boundary. This probe created a larger than normal carbon source, so the plasma formed was composed strongly of fully stripped carbon ions ($6n_{C^{6+}} > n_{D^+}$). This carbon dominated discharge represents a case where the plasma composition is well known because the numerous C^{6+} ions leave little room for any other ions. The consistency between Z_{eff} from CER analysis and VB analysis shown in Fig. 2(c) demonstrates that this analysis is able to determine plasma impurity content for a wide range of Z_{eff} values, and not just standard L-mode and H-mode discharges. It is noteworthy that for this discharge all but one of the HFS VB measurements saturated, making verification of flux symmetry impossible. However, all C^{6+} density measurements were on the LFS, meaning that both Z_{eff} profiles only observed the outer midplane of the tokamak.

In the future, this plasma composition analysis will be used for routine determination of the plasma Z_{eff}, verifying absolute and relative diagnostic calibrations, and supporting power and exhaust studies utilizing impurity seeding.

Acknowledgments

This material is based on work supported by the U.S. Department of Energy, Office of Science, Office of Fusion Energy Sciences, using the DIII-D National Fusion Facility, a DOE Office of Science user facility under Grants No. DE-FC02-04ER54698, No. DE-AC02-09CH11466, and No. DE-AC05-00OR22725. The author gratefully acknowledges useful discussions with Dr. M. Van Zeeland, Dr. K. Burrell, Dr. T. Ostrcil, Dr. R. McWilliams, Dr. L. Stagner, and Dr. J. Boedo.

References

[1] Silvia Espinosa and Peter J. Catto. Pedestal radial flux measuring method to prevent impurity accumulation. *Physics of Plasmas*, 24(5):055904, May 2017.

[2] B.W Rice and E.B Hooper. Poloidal field measurements during sawteeth and disruptions on MTX. *Nuclear Fusion*, 34(1):1–21, January 1994.

[3] R. Valencia, G. Olayo, G. Cruz, R. Lopez, E. Chavez, L. Melendez, A. Flores, and E. Gaytan. Estimation of Zeff in Novillo Tokamak. *Journal of Nuclear Materials*, 228(2):254–256, March 1996.

[4] K. Kadota, M. Otsuka, and J. Fujita. Space- and time-resolved study of impurities by visible spectroscopy in the high-density regime of JIPP T-II tokamak plasma. *Nuclear Fusion*, 20(2):209–212, February 1980.

[5] D.G Whyte, M.R Wade, D.F Finkenthal, K.H Burrell, P Monier-Garbet, B.W Rice, D.P Schissel, W.P West, and R.D Wood. Measurement and verification of z_{eff} radial profiles using charge exchange recombination spectroscopy on DIII-D. *Nuclear Fusion*, 38(3):387–398, March 1998.

[6] S. Von Goeler, W. Stodiek, H. Eubank, H. Fishman, S. Grebenshchikov, and E. Hinnov. Thermal X-ray spectra and impurities in the ST Tokamak. *Nuclear Fusion*, 15(2):301–311, April 1975.

[7] D. P. Schissel, R. E. Stockdale, H. St. John, and W. M. Tang. Measurements and implications of Zeff profiles on the DIII-D tokamak. *Physics of Fluids*, 31(12):3738, 1988.

[8] M A Van Zeeland, J H Yu, N H Brooks, W W Heidbrink, K H Burrell, R J Groebner, A W Hyatt, T C Luce, N Pablant, W M Solomon, and M R Wade. Active and passive spectroscopic imaging in the DIII-D tokamak. *Plasma Physics and Controlled Fusion*, 52(4):045006, April 2010.

[9] N. C. Logan, B. A. Grierson, S. R. Haskey, S. P. Smith, O. Meneghini, and D. Eldon. OMFIT Tokamak Profile Data Fitting and Physics Analysis. *Fusion Science and Technology*, 74(1-2):125–134, August 2018.

[10] E. S. Marmar, R. L. Boivin, R. S. Granetz, J. W. Hughes, B. Lipschultz, S. McCool, D. Mossessian, C. S. Pitcher, J. E. Rice, and J. L. Terry. High resolution visible continuum imaging diagnostic on the Alcator C-Mod tokamak. *Review of Scientific Instruments*, 72(1):940–943, January 2001.

[11] A. Patel, P. G. Carolan, N. J. Conway, and R. J. Akers. Zeff profile measurements from bremsstrahlung imaging in the MAST spherical tokamak. *Review of Scientific Instruments*, 75(11):4944–4950, November 2004.

[12] H. Meister, R. Fischer, L. D. Horton, C. F. Maggi, D. Nishijima, C. Giroud, K.-D. Zastrow, B. Zaniol, ASDEX Upgrade Team, and JET-EFDA Contributors. Zeff from spectroscopic bremsstrahlung measurements at ASDEX Upgrade and JET. *Review of Scientific Instruments*, 75(10):4097–4099, October 2004.

[13] H. Meister, R. Dux, L. D. Horton, B. Kurzan, H. Zohm, the ASDEX Upgrade Team, and P. J. McCarthy. An integrated system to measure the effective charge of fusion plasmas in the ASDEX Upgrade tokamak. *Review of Scientific Instruments*, 74(11):4625–4633, November 2003.

[14] Hans Hormann. Temperaturverteilung und Elektronendichte in frei brennenden Lichtbogen. *Zeitschrift fur Physik*, 97(9):539–560, September 1935.

[15] Shigeru Morita and Jurgen Baldzuhn. Zeff measurement and analysis of reheat-mode discharges in W7-AS. *Max-Planck-Institut fur Plasmaphysik*, 1994.

[16] Abraham. Savitzky and M. J. E. Golay. Smoothing and Differentiation of Data by Simplified Least Squares Procedures. *Analytical Chemistry*, 36(8):1627–1639, July 1964.

[17] M. L. Reinke, I. H. Hutchinson, J. E. Rice, M. Greenwald, N. T. Howard, A. Hubbard, J. W. Hughes, J. L. Terry, and S. M. Wolfe. Parallel transport studies of high-Z impurities in the core of Alcator C-Mod plasmas. *Physics of Plasmas*, 20(5):056109, May 2013.

[18] Matthew Newville, Till Stensitzki, Daniel B. Allen, Michal Rawlik, Antonino Ingargiola, and Andrew Nelson. Lmfit: Non-Linear Least-Square Minimization and Curve-Fitting for Python. *Astrophysics Source Code Library*, page ascl:1606.014, June 2016.